

University of Texas Rio Grande Valley

ScholarWorks @ UTRGV

Physics and Astronomy Faculty Publications
and Presentations

College of Sciences

1998

Ab initio single- and multiple-scattering EXAFS Debye-Waller factors: Raman and infrared data

Nicholas Dimakis

The University of Texas Rio Grande Valley

Grant Bunker

Follow this and additional works at: https://scholarworks.utrgv.edu/pa_fac



Part of the [Astrophysics and Astronomy Commons](#), and the [Physics Commons](#)

Recommended Citation

Dimakis, Nicholas and Bunker, Grant, "Ab initio single- and multiple-scattering EXAFS Debye-Waller factors: Raman and infrared data" (1998). *Physics and Astronomy Faculty Publications and Presentations*. 389.

https://scholarworks.utrgv.edu/pa_fac/389

This Article is brought to you for free and open access by the College of Sciences at ScholarWorks @ UTRGV. It has been accepted for inclusion in Physics and Astronomy Faculty Publications and Presentations by an authorized administrator of ScholarWorks @ UTRGV. For more information, please contact justin.white@utrgv.edu, william.flores01@utrgv.edu.

Ab initio single- and multiple-scattering EXAFS Debye-Waller factors: Raman and infrared data

Nicholas Dimakis and Grant Bunker
Illinois Institute of Technology, Chicago, Illinois 60616
(Received 23 January 1998)

The extended x-ray-absorption fine structure (EXAFS) Debye-Waller factor is an essential term appearing in the EXAFS equation that accounts for the molecular structural and thermal disorder of a sample. Single- and multiple-scattering Debye-Waller factors must be known accurately to obtain quantitative agreement between theory and experiment. Since the total number of fitting parameters that can be varied is limited in general, data cannot support fitting of all relevant multiple-scattering Debye-Waller factors. Calculation of the Debye-Waller factors is typically done using the correlated Debye approximation, where a single parameter (Debye temperature) is varied. However, this procedure cannot account in general for Debye-Waller factors in materials with heterogeneous bond strengths, such as biomolecules. As an alternative procedure in this work, we calculate them *ab initio* directly from the known or hypothetical three-dimensional structure. In this paper we investigate the adequacy of various computational approaches for calculating vibrational structure within small molecules. Detailed EXAFS results will be presented in a subsequent paper. Analytical expressions are derived for multiple scattering Debye-Waller factors, based on the plane wave approximation. Semiempirical Hamiltonians and the *ab initio* density functional method are used to calculate the normal mode eigenfrequencies and eigenvectors. These data are used to calculate all single- and multiple-scattering Debye-Waller factors up to a four atom cluster. These *ab initio* Debye-Waller factors are compared to those calculated from experimental infrared and Raman frequencies. As an example comparison with experimental EXAFS data from GeCl_4 , GeH_3Cl gases are also reported. Good agreement is observed for all cases tested. [S0163-1829(98)05430-7]

I. INTRODUCTION

X-ray-absorption fine structure (XAFS) spectroscopy^{1,2} is a technique used to provide information regarding structural and electronic composition of a given sample. In XAFS, long-range order is not required, thus crystalline and amorphous materials can be treated on the same basis.

The XAFS Debye-Waller factor is an essential term that appears, in the simplest case, as an exponential of the form $e^{-2k^2\sigma^2}$ in the XAFS $\chi(k)$ equation, and which accounts for the structural and thermal disorder of a given sample. The parameter σ^2 is the mean square variation (MSV) of a given scattering path. The Debye-Waller factor is a k^2 -dependent term; its importance is enhanced as k is increased. For $k \leq 3-4 \text{ \AA}^{-1}$ the effect of this factor on the XAFS $\chi(k)$ is usually minimal and often can be ignored. Unless otherwise stated, in this work, any reference to Debye-Waller factor refers to thermal component only, and at the small disorder limit.

Quantitative analysis of EXAFS spectra requires the ability to determine Debye-Waller factors either experimentally or computationally. Tremendous progress has been made in recent years in calculating the electronic single- and multiple-scattering effects in XAFS.³ However, to date, there has not been a corresponding improvement in calculating vibrational properties which are also critical for obtaining quantitative agreement with XAFS spectra. The focus of this work is *ab initio* calculation of Debye-Waller factors, particularly for situations in which it is impossible to determine all relevant Debye-Waller factors by fitting data. This potentially extends the range and power of the XAFS technique by

eliminating the need to fit more parameters than data can realistically support.

When experimental EXAFS data are available, calculation of the Debye-Waller factor for single-scattering paths is typically done as follows: experimental $\chi(k)$ data are fitted with computationally simulated $\chi(k)$, using scattering amplitudes and phases obtained from compounds of known structure. Fitting is done by nonlinear least squares methods, and simulation is obtained using theoretical calculations or empirical standards.

When experimental EXAFS data are *not* available, single-scattering Debye-Waller factors can be estimated by the FEFF6 program,⁴ using either the Debye or Einstein approximations. Both are single-parameter models, depending upon Debye and Einstein temperature, respectively. These models have advantages and disadvantages, but they can be accurate enough when bonds of homogeneous strength are involved.

Single-scattering Debye-Waller factors normally are determined from experimental data, but only as an average over "shells" of atoms. In most cases it is not possible to determine σ^2 for all individual single-scattering paths. Furthermore the number of important multiple-scattering paths may number in the hundreds, so it becomes hopeless to determine all of them by fitting. It can be shown that the maximum number of independent parameters determinable from XAFS is $2\Delta k\Delta R/\pi \approx 20-30$ where Δk and ΔR are the useful k - and R -space data ranges.

Single scattering and two-atom multiple scattering are not the only types of scattering appearing in the EXAFS spectrum. Usually, three- and sometimes four-atom, or even higher multiple-scattering paths also may be significant. The relative importance of the multiple scattering depends upon

the structure of the specific sample. If the scattering angle defined by the central absorber, the first scatterer, and the second scatterer is less than 140° – 150° , three-atom scattering is confined predominantly to the near-edge (XANES) region where, as discussed before, Debye-Waller factors are usually not important. But as this angle approaches 180° (linear molecules), multiple scattering is greatly enhanced and affects also the EXAFS region. This is called the “focusing” effect. In highly symmetric systems large angle multiple scattering may also be important in the EXAFS region.

Whenever the focusing effect is present, contributions from multiple-scattering paths *must* be included in the EXAFS equation. Because of the large number of fitting parameters that would be required and the limited information content of EXAFS spectra, multiple-scattering Debye-Waller factors cannot be obtained by the fitting technique. However, viable alternatives include calculation of these parameters by either an approximated model, by a full normal mode analysis, by equation of motion methods, molecular dynamics, or other methods.

As mentioned before, both Debye and Einstein approximations are single-parameter models. These methods permit one to calculate the σ^2 of a single-scattering path only when all bonds are equivalent, or may be approximated by a suitable average. In appropriate systems these models can provide accurate results. However, in systems that involve highly anisotropic bonds, e.g., strong bonds in a plane and weak bonds along the perpendicular axis, as in aromatic rings in amino acid residues, or high- T_c superconductors, or Jahn-Teller distorted transition metal coordination complexes, neither of these models are able to accurately calculate *all* single-scattering Debye-Waller factors. This is exactly the situation for a typical three-atom multiple-scattering path: strong bonds (stretching) are vibrationally coupled with various weaker bonds (bending, and sometimes other deformations). Therefore neither of these two approximations should be used for three- and/or four-atom multiple-scattering Debye-Waller factor calculations in such systems.

One approach to estimate these parameters is by means of a normal mode analysis using force constants obtained from various force field models, or better yet, to calculate them for specific structure under consideration. We have tried some tabulated force field models and found them to be insufficiently accurate for our purposes.⁵ Alternatively, calculation of force constants can be done by a variety of self-consistent quantum chemical methods that are available, which is the approach used in this work. These methods may be divided into two main categories: the *ab initio* and the semiempirical approaches. The essential difference between *ab initio* and semiempirical methods is that, in the latter, some of these integrals are approximated using experimental results for calibration. This makes semiempirical methods much faster, approximately 10^3 times, than *ab initio*, but also less flexible and accurate.

A question that arises here is why the FEFF7 program cannot be used to perform a molecular *ab initio* normal mode analysis. The answer is simple: FEFF7 is *not* a molecular self-consistent field method and cannot be used to provide any information regarding the chemical structure of a molecule. This is why FEFF7, in order to calculate Debye-Waller fac-

tors, uses the Debye model which does not require any extensive force constant calculation beforehand, except for a single force constant (Debye temperature) provided by the user. Ideally force constants would be generated by a SCF version of the multiple scattering EXAFS codes. Until such codes become available, the approach presented here is practical for molecular systems.

In this work quantum-mechanical molecular calculation of force field constants and normal mode analysis is done by the use of the semiempirical Hamiltonians AM1 (Ref. 6) and MNDO (Ref. 7) and the *ab initio* density functional method (DFT).⁸ These, among others, calculate the normal mode eigenfrequencies and eigenvectors of a particular molecule, which in turn is used for calculation of MSV parameters. Semiempirical methods do *not* work well for every material, but they can be accurate enough for the same purposes when they are applied to organic samples. Since their execution time is only a fraction that of any *ab initio* method they can be used on large organics, e.g., biomolecules, where a DFT, on ordinary 1997 era workstations, may be impractical. We expect this limitation to disappear as the cost of computing power decreases. If the speed of computers doubles every two years and the time of execution scales as N^3 , where N is the number of atoms in the cluster, then the cluster size practically will double every six years. Algorithmic improvements are also feasible.

Density functional methods are preferred over the Hartree-Fock method^{9,10} because they account approximately for both electron exchange and correlation terms. They require almost the same amount of CPU time as the Hartree-Fock method, but the inclusion of the electron correlation term and its various nonlocal density approximations make it suitable for a broad range of materials. Even when very weak bonds are present, e.g., hydrogen bonds, the addition of a term dependent on the derivative of the electron density to the molecular energy will systematically improve the results. This is one example of what are called nonlocal corrections but, with the exception of the F_2 molecule, are not used here. In general, for weak bonds or high temperatures, anharmonic effects will be important and the methods described here would need to be extended. For the systems of primary concern here, which involve strong covalent bonds, anharmonic effects are neglected. Other means of approximating an anharmonic potential is by the use of the quasiharmonic method and is not discussed here. DFT provides a good balance of accuracy, flexibility, and execution speed. It is also preferred over the more accurate but much slower second or fourth order Møller-Plesset perturbation methods referred to as MP2 and MP4, respectively.¹¹

The accuracy of the density functional method used here depends, as almost other *ab initio* methods, on the basis functions. In this work, the more extensive Gaussian basis set, where available, has been used.

A variety of inorganic and organic molecules were chosen to estimate the accuracy of the various quantum chemistry codes used. Diatomic molecules are examined first, triatomic and tetra-atomic inorganic structures follow. Aromatic and nonaromatic organic structures are examined separately since they usually appear in biomolecules, e.g., in amino acids and nucleotides, which are of particular interest to us. In this work we have continued on attention to noncrystalline mo-

lecular systems, but the method should also work in crystals, using appropriate programs.

Theoretical $\chi(k)$ data using σ^2 from semiempirical and density functional methods are matched with computationally calculated σ^2 using experimental infrared and Raman spectra. This is because the accuracy of the σ^2 depend mainly on how well the normal mode frequencies are estimated. Future work also include comparison with experimental EXAFS data. The density functional method proves to be a broadly applicable material method whereas semiempirical AM1 and MNDO are limited to organic materials only. Some exceptions to this statement are also described.

The multiple-scattering Debye-Waller factor problem represents an attempt to directly address the problem by means of a self-consistent approach. Recently Poiarkova and Rehr¹² presented an alternative method using the ‘‘equation of motion’’ method, which involves Fourier transformation of the time dependence of the molecular dynamics. They use *tabulated* force constants to calculate the corresponding σ^2 . The accuracy of this method depends on how well the tabulated force constants resemble the actual ones. Clearly, reliance on tabulated force constants lacks self-consistency, so that, by its nature, chemical differences in bond strength are not accurately taken into account. The normal mode frequency varies among different structures containing a particular bond. Because tabulated bond strengths depend solely on the particular type of atom-atom bond, they cannot account for chemical variation in bond strength.

II. THEORY

A. Two-atom multiple scattering

The EXAFS equation, in the plane wave approximation, accounting for the two atom multiple scattering is written as

$$\chi(k) = \sum_{l=1}^{\infty} \chi_{2l}(k), \quad (1)$$

where $\chi_{2l}(k)$ denotes $n\text{legs}=2l$ scattering. Generally speaking any $2l$ scattering will produce a backscattered wave of the form

$$\frac{T^{2l}}{k|\vec{R}_i^{2l}|} e^{\overbrace{2i\vec{k} \cdot \vec{R}'_i + \dots + 2i\vec{k} \cdot \vec{R}'_i}_{l \text{ times}}} \quad (2)$$

where $T^{2l}(k)$ is the scattering amplitude for the $2l$ path. The exponential term includes all phase factors that account for the variation of the atomic potential. The instantaneous distances \vec{R}'_i are defined as

$$\vec{R}'_i = \vec{u}_i - \vec{u}_0 + \vec{R}_i, \quad (3)$$

where \vec{u}_i are the displacement vectors from the equilibrium positions \vec{R}_i , \vec{u}_0 is the displacement vector of the central absorber. Distances \vec{R}'_i that occur in the denominator of Eq. (2) may be replaced with the corresponding equilibrium values \vec{R}_i . The magnitude of the instantaneous vector position \vec{R}'_i is approximated as

$$|\vec{R}'_i| \simeq |\vec{R}_i^2 + 2\hat{R}_i(\vec{u}_i - \vec{u}_0)|^{1/2} \simeq |\vec{R}_i| + \hat{R}_i(\vec{u}_i - \vec{u}_0), \quad (4)$$

where \hat{R}_i denotes the unit vector in the direction of \vec{R}_i . Therefore the exponential factor in Eq. (2) may be written as

$$e^{2i\vec{k} \cdot \vec{R}'_i} \simeq e^{2i\vec{k} \cdot \vec{R}_i} e^{2i\hat{R}_i(\vec{u}_i - \vec{u}_0)}. \quad (5)$$

and by thermally averaging the second exponential factor we have

$$\langle e^{2i\hat{R}_i(\vec{u}_i - \vec{u}_0)} \rangle = e^{-2k^2 l^2 \langle (\hat{R}_i(\vec{u}_i - \vec{u}_0))^2 \rangle}. \quad (6)$$

Therefore the two-atom multiple-scattering Debye-Waller factor for any $n\text{legs}=2l$ is written in terms of the $\sigma_{i,SS}^2$ single-scattering factor Debye-Waller factor as

$$\sigma_i^2(2l) = l^2 \sigma_{i,SS}^2. \quad (7)$$

B. Three-atom multiple scattering

Consider a three atom cluster and a $n\text{legs}=l$ multiple scattering path with $n\text{legs}=\alpha$ from the absorber 0 to atom i , $n\text{legs}=\beta$ from i to j , and $n\text{legs}=\gamma$ from j back to 0, such that

$$l = \alpha + \beta + \gamma. \quad (8)$$

Following a similar discussion as in Sec. II A the backscattered wave amplitude of such a path is proportional to

$$\frac{T(\theta_i, \phi_i) T(\theta_j, \phi_j)}{k|\vec{R}_{0i}|^\alpha |\vec{R}_{0j}|^\gamma |\vec{R}_{ij}|^\beta} e^{(i\alpha\vec{k}_i \cdot \vec{R}'_i + i\gamma\vec{k}_j \cdot \vec{R}'_j + i\beta\vec{k}_{ij} \cdot \vec{R}'_{ij})}. \quad (9)$$

Using Eq. (4) the exponential factor in the last equation becomes

$$\begin{aligned} & e^{(i\alpha\vec{k}_i \cdot \vec{R}'_i + i\gamma\vec{k}_j \cdot \vec{R}'_j + i\beta\vec{k}_{ij} \cdot \vec{R}'_{ij})} \\ & \simeq e^{ik(\alpha|\vec{R}_i| + \gamma|\vec{R}_j| + \beta|\vec{R}_{ij}|)} \\ & \times e^{ik[\alpha\hat{R}_i(\vec{u}_i - \vec{u}_0) + \gamma\hat{R}_j(\vec{u}_j - \vec{u}_0) + \beta\hat{R}_{ij}(\vec{u}_i - \vec{u}_j)]}. \end{aligned} \quad (10)$$

A thermal average of the second exponential factor leads to the MSV σ^2 , expressed as

$$\sigma^2 = \frac{1}{2} \sum_n [\alpha p'_{0i}(n) + \beta p'_{ij}(n) + \gamma p'_{j0}(n)]^2 \langle Q_n^2 \rangle, \quad (11)$$

where $p'_{ij}(n)$ are defined by

$$p'_{ij}(n) = \frac{\hat{R}_{ij} \cdot \vec{\epsilon}_i(n)}{\sqrt{m_i}} - \frac{\hat{R}_{ij} \cdot \vec{\epsilon}_j(n)}{\sqrt{m_j}}. \quad (12)$$

$\epsilon_i(n)$ are the normal mode eigenvectors, m_i mass of the i th atom in the cluster, and $\langle Q_n^2 \rangle$ is

$$\langle Q_n^2 \rangle = \frac{\hbar}{2\omega_n} \coth\left(\frac{\hbar\omega_n}{2K_B T}\right). \quad (13)$$

C. Four-atom multiple scattering

Four-atom multiple scattering is generally the highest cluster multiple scattering to be examined. This is because a path involving more than three scattering atoms tends to be

TABLE I. Calculated single-scattering EXAFS σ^2 for diatomic gases.

Molecule	$\sigma^2, 10^{-3} \times \text{\AA}^2$			Exp
	AM1	MNDO	DFT	
Br ₂	1.345	1.286	2.281	2.064
O ₂	1.007	0.851	1.497	1.356
N ₂	0.871	0.878	1.067	1.033
F ₂ ^a	1.303	1.048	2.227	2.191
Cl ₂	1.261	1.416	2.215	1.974
CO	1.083	1.031	1.118	1.147
FCI	1.288	1.317	1.873	1.848
NO	0.932	0.867	1.150	1.202
ClBr	1.334	1.343	2.171	1.940
BrF	1.363	1.217	1.873	1.710

^aBecke nonlocal correction has been used.

of a much lower probability due to larger effective path length involved. When focusing effect takes place, four-atom multiple scattering up to $n\text{legs}=6$ can be observed not only in the XANES but also in the EXAFS region of the spectrum. A general formula for a four-atom $n\text{legs}=l$ multiple scattering is given by

$$\sigma^2 = \frac{1}{2} \sum_n [\alpha p'_{0i}(n) + \beta p'_{ij}(n) + \gamma p'_{jk}(n) + \delta p'_{k0}(n)]^2 \langle Q_n^2 \rangle, \quad (14)$$

where $\alpha + \beta + \gamma + \delta = l$.

III. PROCEDURE

With the exception of the GeCl₄, GeH₃Cl all other model samples being presented in this work were built using the MOLECULAR EDITOR Ver. 3.8 by CAChe Scientific, now part of Oxford Molecular Group. Their structure was optimized by minimizing the quantum-mechanically calculated energy using either the AM1, MNDO (MOPAC package by CAChe), or DFT method (MULLIKEN package by IBM). Normal mode analysis, using the same methods, was also performed. GeCl₄, GeH₃Cl were built and analyzed with UNICHEM version 4.0 by Oxford Molecular Group. UNICHEM has the option of using a double zeta (DZ) (Ref. 20) basis set that tend to give more accurate results than the Popple basis set used by Mulliken. Auxiliary basis set A1 was also used.

A program written by the authors reads normal mode eigenfrequencies and eigenvectors and calculates σ^2 for all single- and multiple-scattering paths up to eight number of legs. Since the number of multiple-scattering paths might be in the hundreds, our program reads a path.dat and a files.dat file produced by FEFF7 for the same structure, assigns σ^2 for the corresponding path, and automatically saves them on the files.dat file. By rerunning FEFF7 using this new files.dat file $\chi(k)$ data that include Debye-Waller factors are obtained.

IV. RESULTS AND DISCUSSION

In this section results from DFT and semiempirical methods are compared with results from IR and Raman frequencies. The experimental Debye-Waller factors, shown in the

TABLE II. Calculated single-scattering EXAFS σ^2 for triatomic and tetra-atomic molecules.

Molecule	$\sigma^2, 10^{-3} \times \text{\AA}^2$			Exp
	AM1	MNDO	DFT	
F ₂ O	1.724	1.230	2.255	2.314
CO ₂	1.110	1.074	1.170	1.214
SO ₂	1.613	1.138	1.296	1.250
SO ₃	1.367	1.245	1.281	1.230
O=CCl ₂ ^a	1.216	1.135	1.326	1.364
^b	2.264	2.858	2.641	2.528
S=CF ₂ ^c	1.820	1.475	1.512	1.529
^d	1.595	1.398	1.863	1.913
O=CCIF ^a	1.209	1.160	1.262	1.306
^d	1.581	1.402	1.916	1.926
^b	2.162	1.918	2.537	2.467

^aC=O.

^bC—C.

^cC=S.

^dC—F.

tables, were derived by substituting the corresponding IR and Raman frequencies to a MOPAC file.

A. Diatomic gases

In order to make a first test regarding the accuracy of the semiempirical AM1, MNDO, and the *ab initio* DFT method, ten diatomic molecules are examined. Diatomic molecules have only one normal vibrational mode, which is a purely stretching vibration, and therefore their single-scattering σ^2 comes only from one frequency. Therefore the accuracy of each method depends only on how well this normal mode frequency approaches the experimental value.

Single-scattering σ^2 of five A-A type diatomic molecules Br₂, O₂, N₂, F₂, Cl₂, and five A-B molecules are presented in Table I. All experimental frequencies¹³ *do* include anharmonicity, and have been recorded by spectrometers. This anharmonicity shifts the harmonic frequency by a few cm⁻¹ but special attention has to be given to the F₂ where a downshift of approximately 180 cm⁻¹ has been observed. In order to overcome this difficulty, a Becke nonlocal correction was included on the DFT runs. There was no equivalent correction for the semiempirical methods. All other molecules are treated without nonlocal corrections.

By examining Table I, in the A-A case, DFT relative error ranges from 10.8% (Cl₂) to 1.6% (F₂) where in the A-B case the corresponding range is from 10.6% (ClBr) to 1.3% (FCI). Therefore in case of diatomic gases, with the exception of CO whereas semi-empirical methods also provide accurate results, for best accuracy, single-scattering Debye-Waller factors should be calculated using the DFT method. Since all multiple-scattering paths on two atom systems depend on this one normal mode frequency, the above statement is relevant for their multiple-scattering Debye-Waller factors as well.

B. Single scattering

1. Triatomic and tetraatomic molecules

The triatomic F₂O, CO₂, SO₂ and the tetraatomic SO₃, O=CCl₂, S=CF₂, O=CCIF are the next to be

TABLE III. Calculated single-scattering EXAFS σ^2 for organic nonaromatic samples.

Molecule	$\sigma^2, 10^{-3} \times \text{\AA}^2$			Exp
	AM1	MNDO	DFT	
CH ₃ Cl	2.268	2.075	2.586	2.601
HC≡CH	1.205	1.220	1.289	1.322
H ₃ CCN ^a	1.800	1.830	2.086	2.175
^b	2.017	2.070	2.379	2.502
H ₂ C=C=O ^a	1.458	1.507	1.675	1.702
^b	1.729	1.746	1.950	1.954
H ₂ C≡CCH ₃ ^d	1.196	1.208	1.298	1.329
^b	2.122	2.157	2.486	2.547

^aFirst C is the central absorber.

^bSS second shell, where all hydrogens are ignored.

examined.¹³ From now on, discussion of the single scattering is separated from the multiple scattering. As the number of atoms in a molecule is increased, an accurate single-scattering Debye-Waller factor does *not* guarantee accurate multiple-scattering Debye-Waller factor, as in the case of diatomic molecules. This is mainly due to the fact that in the three- and four-atom multiple scattering, various stretching and bending modes appear in the spectrum. In order to obtain accurate results for *all* scattering paths, only a “variety” of frequencies is actually needed. By “variety” we mean that a precise description of the complete spectrum of poluatomic molecule is *not* always necessary.

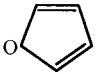
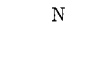
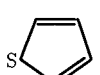

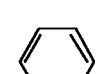

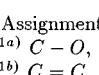
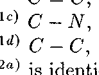
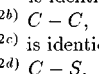
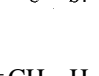
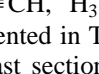
Wherever referenced carbon is taken to be the central absorbing atom. This is mainly for the following reason: since the main purpose of this work is to treat organic rings similar to aminoacid side groups, we examine the behavior of how well bending and/or stretching of organic bonds is estimated using the semiempirical or DFT method. In practice carbon is rarely chosen as an absorbing atom in an EXAFS experiment. This is because its *K* edge is 284.2 eV relatively low compared to the keV range of most of the experiments done today. Also in case of an organic sample with an *unknown* geometry, since more than one C atom will be absorber and scatterer, there is no way of determining positions or angles of atoms in such a molecule.

Similarly, as in the diatomic molecules, by examining Table II, the DFT relative error ranges from 4.27% (O = CCl₂, C-Cl assignment) to 0.52% (O = CClF, C-Cl assignment). Therefore regarding inorganic molecular samples (at least up to tetra-atomic molecules), DFT is accurate enough for the calculation of the single scattering and two-atom multiple-scattering Debye-Waller factors whereas the use of semiempirical methods is discouraged. This is a general statement and exceptions to this rule, as in case of the MNDO calculation of the Debye-Waller factor in SO₃, might occur.

2. Nonaromatic molecules

Organic nonaromatic molecules are next to be examined. Organic molecules are the main purpose of this work, especially aromatic molecules that appear on protein structure. Aromatic structures are examined in Sec. III B 3. Single scattering σ^2 of five nonaromatic molecules CH₃Cl, HC

TABLE IV. Calculated single-scattering EXAFS σ^2 for aromatic samples. Central absorber is the upper left carbon for the first ring and the upper right for the second ring. Rows denote shells.

Molecule*	$\sigma^2, 10^{-3} \times \text{\AA}^2$			
	AM1	MNDO	DFT	Exp
 (1a)	1.952	1.682	1.860	1.845
 (1b)	1.713	1.763	1.988	1.960
 (1c)	2.293	2.214	2.340	2.333
 (1d)	2.331	2.481	2.608	2.678
 (2a)	1.742	1.719	1.894	1.927
 (2b)	1.943	2.018	2.110	2.109
 (2c)	2.538	2.781	2.697	2.709
 (2d)	2.366	2.390	2.506	2.508
 (3)	1.833	1.949	1.978	2.009
 (4)	2.651	2.841	2.983	2.942
 (5)	3.406	3.630	3.939	3.856

* Assignments as follows:

- (1a) C - O,
- (1b) C = C,
- (1c) C - N,
- (1d) C - C,
- (2a) is identical to (1b),
- (2b) C - C,
- (2c) is identical to (1d),
- (2d) C - S.

≡CH, H₃CCN, H₂C=C=O, and H₂C≡CCH₃, are presented in Table III. For the same reasons as explained in the last section, carbon is taken as the central absorbing atom. When multiple carbons appear on a molecule the first carbon from the left is the absorber.

Inspection of the normal mode frequencies^{14,15} shows that C-H stretching modes occur in a range 3000–3500 cm⁻¹, thus consisting of a “group” of frequencies for this particular vibration. This can also be confirmed for other types of vibrations. If a C-H stretching frequency is set to approximately 3000 cm⁻¹, then the corresponding absolute error induced on the single scattering σ^2 for any C-X path (excluding hydrogens) is negligible. This statement is also valid for multiple scattering. This is because MSV's depend mainly on modes (stretching, bending, or combination of the two) that involve atoms which belong to the same path of interest. Therefore only a certain “group” of the whole spectrum will contribute to the particular Debye-Waller factor.

By examining Table III, MNDO and AM1 provide far more accurate results than for the inorganic case. Specifically, MNDO errors range from 25.34% (CH₃Cl) to 7.91% (HC≡CH), and AM1 errors range from 24.04% (H₃CCN, second shell) to 9.7% (HC≡CH). This is fully expected due to the parametrization of these two semiempirical methods. On the other hand, DFT is still far more accurate but at the cost of much higher CPU time. DFT relative error ranges from 5.17% (H₃CCN, second shell) to 0.2% (H₂C=C=O, second shell).

Therefore, with regard to organic nonaromatic molecular samples, DFT is an accurate approach for the calculation of

TABLE V. Calculated double-scattering EXAFS σ^2 for triatomic and tetra-atomic molecules.

Molecule	$\sigma^2, 10^{-3} \times \text{\AA}^2$			Exp
	AM1	MNDO	DFT	
FO ₂	2.276	1.606	2.715	2.868
CO ₂	1.426	1.373	1.552	1.581
SO ₂	2.585	2.015	2.666	2.542
SO ₃	2.444	2.553	2.442	2.272
O=CCl ₂ ^a	2.185	2.020	2.399	2.348
^b	2.490	2.671	2.185	2.242
S=CF ₂ ^c	2.100	1.828	1.854	1.898
^d	2.037	1.724	2.223	2.257
O=CCIF ^a	2.199	2.687	2.294	2.225
^e	1.780	1.642	1.828	1.810
^f	2.297	2.128	2.141	2.083

^aC—Cl—O—C.^bC—Cl—Cl—C.^cC—F—S—C.^dC—F—F—C.^eC—F—O—C.^fC—F—Cl—C.

the single-scattering and two-atom multiple-scattering Debye-Waller factors. The semiempirical methods can be used to provide a fast first estimation of the σ^2 's.

3. Aromatic molecules

Next we examine aromatic (ring) molecules under the single-scattering scheme. Two five member rings and one six member (benzene) are discussed.

Nonplanar normal mode vibrations^{15,16} tend to play no significant role in the Debye-Waller factor calculation. This is because these modes do not contribute to the planar MSV σ^2 single or multiple scattering, thus allowing us, arbitrary, to set them equal to any nonzero value. This is also true for some nonaromatic molecules on Sec. IV D but special care must be taken there since there sometimes is no clear definition of a molecular plane.

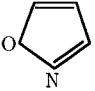
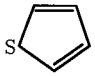

Semiempirical methods, as in the last section, provide very good results for the aromatic molecules as well. In Table IV, the MNDO error ranges from 12.1% (second ring, first shell) to 3.07% (benzene, first shell), and AM1 error ranges from 14.4% (first ring, second shell) to 1.7% (first ring, third shell). The DFT method errors ranges from 3% (second ring, third shell) to an extremely small 0.05% (second ring, second shell). A peculiar result, as in Sec. IV C, also appears here: the semiempirical AM1 provides a better result than the *ab initio* DFT for the third shell of the second ring. For reasons similar to these discussed before, such a peculiarity might also occur for other molecules.

All Debye-Waller factors calculated in this work, refer to nominal "room" temperature, i.e., $T=300$ K. The methods used are expected to be adequate at temperatures for which interatomic potentials are harmonic, including temperatures at which the dominant contribution is quantize zero-point motion.

C. Multiple scattering

Similar to single scattering, double scattering MSV's for all triatomics and tetraatomic inorganic molecules, are given

TABLE VI. Calculated double-scattering EXAFS σ^2 for aromatic molecules.

Molecule*	$\sigma^2, 10^3 \times \text{\AA}^2$				
	AM1	MNDO	DFT	Exp	
	(1a)	1.975	1.949	2.135	2.129
	(1b)	2.185	1.976	2.290	2.217
	(1c)	2.100	2.157	2.475	2.416
	(1d)	2.165	2.221	2.356	2.390
	(1e)	2.211	2.231	2.403	2.398
	(1f)	2.138	2.159	2.293	2.296
	(2a)	2.151	2.295	2.329	2.334
	(2b)	2.150	2.293	2.328	2.334
	(2c)	2.563	2.727	2.674	2.688
	(2d)	2.184	2.027	2.283	2.292
	(2e)	2.349	2.343	2.533	2.523
	(2f)	2.602	2.494	2.741	2.745
	(3a)	2.197	2.329	2.496	2.496
	(3b)	2.873	3.051	3.333	3.313
	(3c)	2.198	2.328	2.498	2.498

* Paths as follows:

(1a) C—O—C (second shell)—C,

(1b) C—O—N—C,

(1c) C—C—C—C,

(1d) C—C (third shell)—N—C,

(1e) C—C (third shell)—O—C,

(1f) C—C (second shell)—N—C,

(2a) C—C (first shell)—C (second shell)—C,

(2b) C—C (third shell)—C (second shell)—C,

(2c) C—C (third shell)—C (first shell)—C,

(2d) C—S—C (first shell)—C,

(2e) C—S—C (second shell)—C,

(2f) C—S—C (third shell)—C,

(3a) C—C (first shell)—C (third shell)—C,

(3b) C—C (second shell)—C (third shell)—C,

(3c) C—C (first shell)—C (first shell)—C.

in Table V. In the CO₂ molecule, one of the two oxygens is set as the absorbing atom, while carbon was the absorber when single scattering was considered. Such a change introduced a shadow effect that, as discussed before, enhances multiple scattering. The DFT relative error is from 6.96% (SO₃) to 0.98% (O=CCIF, C—F—O—C path).

All organic molecules with more than two heavy atoms presented before are also examined. Since, for linear structures, double scattering MSV coincides with the corresponding second shell single scattering σ^2 , MSV's for nonaromatic molecules are not repeated here. For contrast, MSV's for aromatic molecules are given by Table VI. The corre-

TABLE VII. Single-scattering EXAFS MSV σ^2 for GeH₃Cl and GeCl₄ Gases.

Molecule	$\sigma^2, 10^{-3} \times \text{\AA}^2$			Exp.
	AM1	MNDO	DFT	
GeCl ₄	2.203	2.299	2.052	2.070 ^a
GeH ₃ Cl	2.037	2.351	2.833	3.00 ^b

^a $\pm 0.3 \times 10^{-3} \times \text{\AA}^2$.^b $\pm 0.4 \times 10^{-3} \times \text{\AA}^2$.

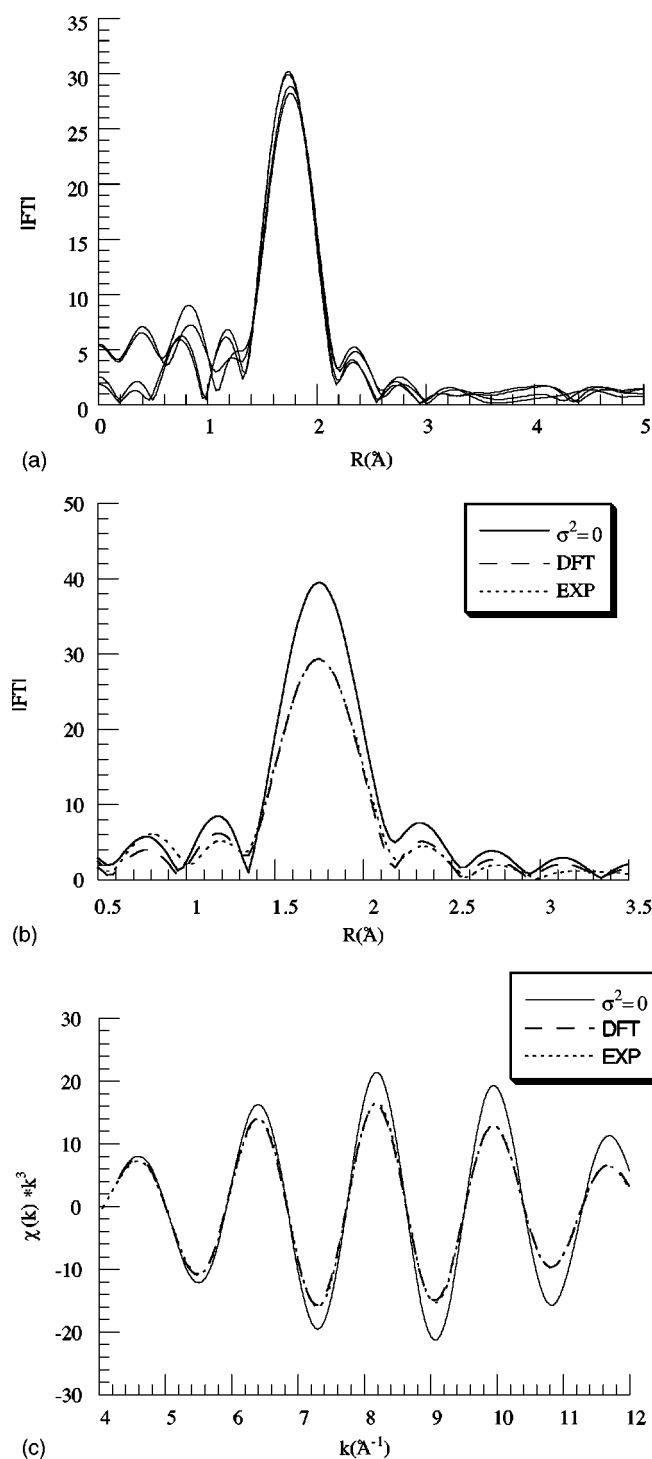


FIG. 1. (a) Four Fourier-transformed experimental EXAFS scans for GeCl₄ gas are plotted to show reproducibility of spectra. Mean experimental (dotted line) vs DFT (dashed line) and $\sigma^2=0$ (solid line) for GeCl₄ gas (b) radial distribution and (c) filtered $\chi(k)$.

sponding DFT error for *all* organic molecules is from 5.17% (H₃CCN) to 0.0% (benzene).

Relative error ranges for the double-scattering case, for either the semiempirical or DFT approximations, remain similar to the corresponding error ranges for the single-scattering case. It is evident that there might be a case in which a method predicts stretching better than bending

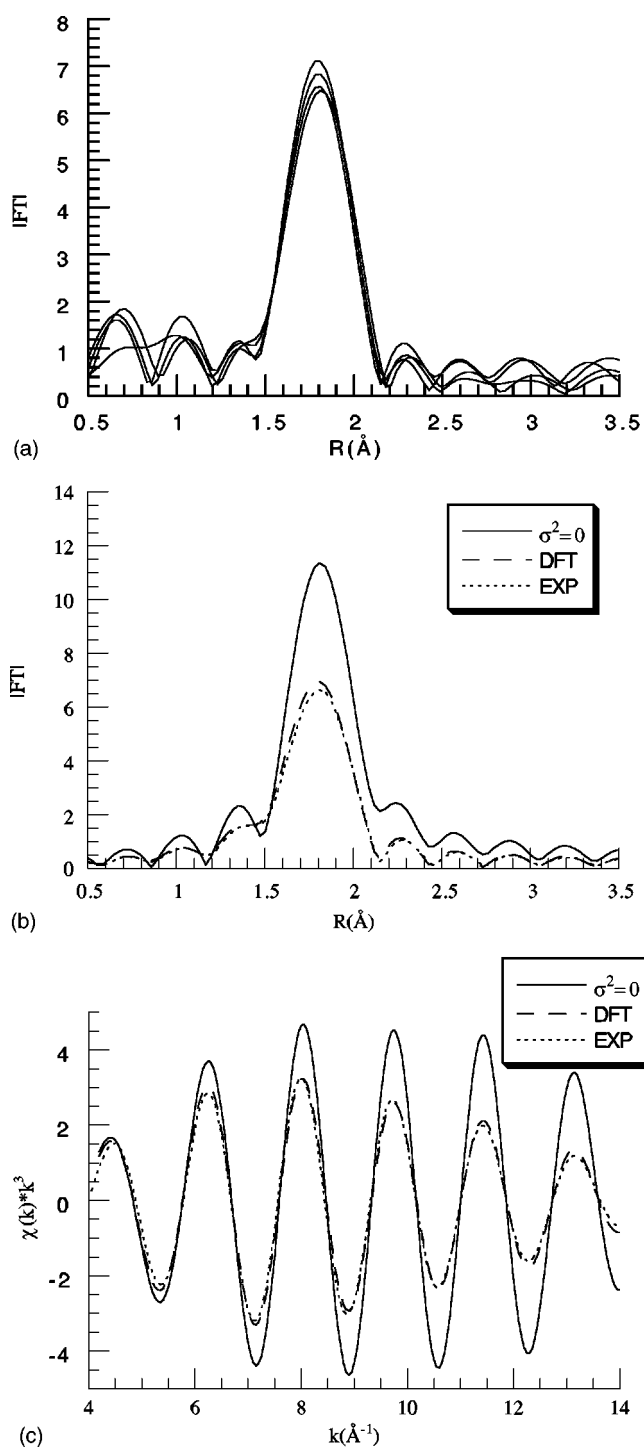


FIG. 2. (a) Four Fourier-transformed experimental EXAFS scans for GeH₃Cl gas are plotted to show reproducibility of spectra. Mean experimental (dotted line) vs DFT (dashed line) and $\sigma^2=0$ (solid line) for GeH₃Cl gas (b) radial distribution and (c) filtered $\chi(k)$.

modes or, vice versa, causing single-scattering MSV's to be predicted accurately enough, but double and some higher order scattering Debye-Waller factors might *not* be in the same error range as the single-scattering ones. Since single scattering is more affected by stretching, and large angle double scattering by bending modes, an acceptable prediction of both guarantees that *all* other three-atom multiple-scattering paths will also be properly predicted.

V. COMPARISON WITH EXPERIMENTAL EXAFS DATA

As an example the methods described above are compared with EXAFS experimental scans. These data refer to GeCl_4 and GeH_3Cl , both gases, taken by Bouldin *et al.*¹⁷ at the National Synchrotron Light Source (NSLS) using the X9-A beamline. Due to the structure of these molecules, multiple scattering is only significant in the XANES area ("wide-angle" multiple scattering). Therefore only single scattering σ^2 , which corresponds to the Ge-Cl path, is reported. Hydrogen scattering in the GeH_3Cl molecule is ignored.

In order to calculate the single-scattering Debye-Waller factor accurately by means of experimental EXAFS scans, more than one scan is required to permit at least a rudimentary statistical analysis. This means that experimental σ^2 will lie on an interval; the less the variation among the scans, the smaller this interval will be. Four experimental $\mu(E)$ scans for each sample are used in this example.

Experimental data analysis is performed as follows. The background is subtracted from the $\mu(E)$ scans.¹⁸ The EXAFS $\chi(k)$ data are calculated from the equation

$$\chi(k) = \frac{\mu(k) - \mu_0(k)}{\Delta\mu}. \quad (15)$$

The background spectrum is normalized by the absorption edge jump $\Delta\mu$ rather than the smooth background μ_0 . This normalization is done in order to avoid severe distortions in the amplitude of the experimental data. However, since theoretical spectra are always normalized by the energy-dependent $\mu_0(k)$, experimental $\chi(k)$ data must be divided by the factor

$$\frac{\Delta\mu^{th}(k)}{\Delta\mu^{th}(k=0)}. \quad (16)$$

This adjustment is called the McMaster correction. The next step is to Fourier transform the $\chi(k)$ data. Any Fourier range can be chosen in this step, but the largest possible is preferred. Any noise contributions due to a larger range can be accounted for later. An optimum range for GeCl_4 is $k \approx 4 \text{ \AA}^{-1}$ – $k \approx 12 \text{ \AA}^{-1}$ while that for GeH_3Cl is $k \approx 4 \text{ \AA}^{-1}$ – $k \approx 14 \text{ \AA}^{-1}$.

The first and only shell (low frequency contributions for hydrogens are excluded from the Fourier transform) is then isolated from any other radial components by an inverse transform. The range of the inverse transform was just sufficient to isolate the desired shell. Theoretical FEFF6 filtered $\chi(k)$ data were matched with experimental $\chi(k)$, using the ratio method¹⁹ and single scattering σ^2 is obtained. It should

be mentioned that theoretical $\chi(k)$ were shifted by -9.5 eV for GeCl_4 and -6.3 eV for GeH_3Cl . This simply reflects monochromator calibration and is of no fundamental significance. This shift was induced *before* the background subtraction and Fourier transform was made; also a Gaussian damping compatible to the experimental σ^2 was introduced in the theoretical $\chi(k)$ data to reduce systematic errors due to Fourier-filtering distortions. Absence of this factor causes a sudden drop of the amplitude of the $\chi(k)$ at the high window end, inducing an absolute error of $\Delta\sigma^2 \approx 0.2 \times 10^{-3} \text{ \AA}^2$ for both samples.

A. The GeCl_4 case

GeCl_4 is examined first. EXAFS experimental Fourier-transformed $\chi(k)$ scans are presented in Fig. 1(a). Since $\Delta\mu^{th}(k=0) \approx 0.62$ the McMaster correction is recommended. The effect of the McMaster correction can be as high as 11% at large k . The inverse-transform range is taken from $R = 1.31 \text{ \AA}$ to $R = 2.14 \text{ \AA}$. Experimental and computationally calculated σ^2 are given by Table VII. A graphical comparison of these results by means of the radial distribution and filtered $\chi(k)$ is given by Figs. 2(b) and 2(c), respectively. The DFT method, under the DZ basis set and A1 auxiliary set provide an accurate estimation of the σ^2 .

B. The GeH_3Cl Case

GeH_3Cl is also examined. Since $\Delta\mu^{th}(k=0) \approx 1$, the McMaster correction is not necessary. Experimental EXAFS Fourier-transformed $\chi(k)$ are presented in Fig. 2(a). Similar to GeCl_4 the inverse-transform range is taken from $R = 1.20 \text{ \AA}$ to $R = 2.15 \text{ \AA}$. Experimental and computationally calculated σ^2 are given by Table VII whereas the Fourier-transformed $\chi(k)$ by Fig. 2(b) and the filtered $\chi(k)$ by Fig. 2(c). The agreement here is even better than expected.

VI. CONCLUSION

Single and multiple-scattering EXAFS MSV's σ^2 were calculated using the semiempirical AM1, MNDO, and the *ab initio* density functional method for a variety of organic and inorganic samples. Expressions for various EXAFS σ^2 multiple-scattering paths were derived from first principles. An *ab initio* calculation of the single and multiple scattering σ^2 is demonstrated and confirmed. This work achieved its goal: to calculate *ab initio* the complete EXAFS spectra including both the electronic and the vibrational aspects via methods presented here of the EXAFS equation. The methods developed are practical for molecular systems and may be generalizable to condensed matter and biological systems.

¹E. A. Stern, in *X-Ray Absorption*, edited by D. C. Koningsberger and R. Prins (Wiley, New York, 1988), Chap. 1.

²P. A. Lee and J. B. Pendry, *Phys. Rev. B* **11**, 2795 (1975).

³J. J. Rehr, R. C. Albers, and S. I. Zabinsky, *Phys. Rev. Lett.* **69**, 3397 (1992).

⁴J. J. Rehr, J. De Leon, S. I. Zabinsky, and R. C. Albers, *J. Am. Chem. Soc.* **113**, 5135 (1991).

⁵N. Dimakis and G. Bunker (unpublished).

⁶M. J. S. Dewar, E. G. Zoebisch, E. F. Healy, and J. P. Stewart, *J. Am. Chem. Soc.* **107**, 3902 (1985).

⁷M. J. S. Dewar and W. Thiel, *J. Am. Chem. Soc.* **99**, 4899 (1977).

⁸R. G. Parr and W. Yang, *Density-Functional Theory of Atoms and Molecules* (Oxford University Press, New York, 1989).

⁹D. R. Hartree, *Proc. Cambridge Philos. Soc.* **24**, 89 (1928).

- ¹⁰V. Fock, Z. Phys. **61**, 126 (1930).
- ¹¹C. Møller and M. S. Plesset, Phys. Rev. **46**, 618 (1934).
- ¹²A. V. Poiarkova and J. J. Rehr (unpublished).
- ¹³K. Nakamoto, *Infrared and Raman Spectra of Inorganic and Coordination Compounds* (Wiley, New York, 1963).
- ¹⁴M. J. S. Dewar and G. P. Ford, J. Am. Chem. Soc. **99**, 1685 (1977).
- ¹⁵T. Shimanouchi, *Tables of Molecular Vibrational Frequencies, National Standard Reference Data Series* (National Bureau of Standards, Washington, D.C., 1972).
- ¹⁶M. J. S. Dewar and G. P. Ford, J. Am. Chem. Soc. **99**, 1685 (1977).
- ¹⁷C. E. Bouldin, G. Bunker, D. A. McKeown, R. A. Forman, and J. J. Ritter, Phys. Rev. B **38**, 10 816 (1988).
- ¹⁸G. Bunker, Ph.D. thesis, University of Washington, 1984.
- ¹⁹D. E. Sayers, E. A. Stern, and F. Lytle, Phys. Rev. Lett. **27**, 1204 (1971).
- ²⁰B. G. Johnson and M. J. Frisch, J. Chem. Phys. **100**, 7429 (1994).